ACS Chemical Neuroscience

pubs.acs.org/chemneuro Research Article

Bcl-2-Homology-Only Proapoptotic Peptides Modulate β-Amyloid Aggregation and Toxicity

Shani Ben-Zichri, Ravit Malishev, Ofek Oren, Daniel N. Bloch, Ran Taube, Niv Papo, and Raz Jelinek*

Cite This: https://doi.org/10.1021/acschemneuro.1c00611 Read Online

ACCESS | Metrics & More | Article Recommendations | Supporting Information

ABSTRACT: Aggregation of the β-Amyloid (Aβ) peptide in brain tissues is the hallmark of Alzheimer's disease (AD). While Aβ is presumed to be insidiously involved in the disease's pathophysiology, concrete mechanisms accounting for the role of Aβ in AD are yet to be deciphered. While Aβ has been primarily identified in the extracellular space, the peptide also accumulates in cellular compartments such as mitochondria and lysosomes and impairs cellular functions. Here, we show that prominent proapoptotic peptides associated with the mitochondrial outer membrane, the Bcl-2-homology-only peptides BID, PUMA, and NOXA, exert significant and divergent effects upon aggregation, cytotoxicity, and membrane interactions of Aβ42, the main Aβ homolog. Interestingly, we show that BID and PUMA accelerated aggregation of Aβ42, reduced Aβ42-induced toxicity and mitochondrial disfunction, and inhibited Aβ42-membrane interactions. In contrast, NOXA exhibited opposite effects, reducing Aβ42 fibril formation, affecting more pronounced apoptotic effects and mitochondrial disfunction, and enhancing membrane interactions of Aβ42. The effects of BID, PUMA, and NOXA upon the Aβ42 structure and toxicity may be linked to its biological properties and affect pathophysiological features of AD.

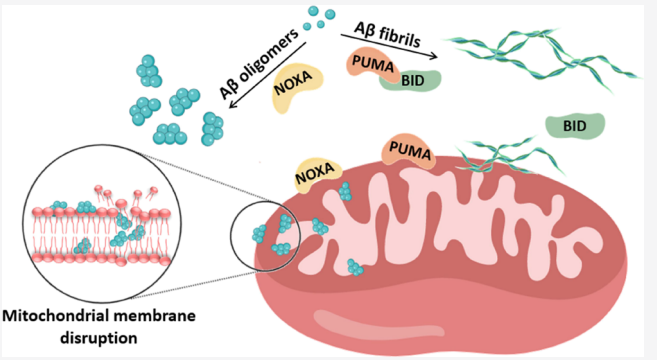

KEYWORDS: *Alzheimer's disease (AD), amyloid β (Aβ), Bcl-2 homology 3 (BH3) peptides, apoptosis, mitochondrial membranes*

1. INTRODUCTION

β-Amyloid (Aβ) is produced through the proteolytic activities of β-secretase and γ-secretase which cleave the amyloid precursor protein (APP).[1,2] Aggregation and accumulation of Aβ in the brains of Alzheimer's disease (AD) patients is a hallmark of the disease and is believed to constitute a major neurodegeneration determinant.[3−5] In parallel, various strategies have been developed to inhibit or remove amyloid deposits.[6,7] However, the mechanism by which Aβ exerts its putative cytotoxic effects is still unknown. While Aβ fibrils are the predominant pathological observation associated with AD, many studies have reported that Aβ oligomers and prefibrillar species are the actual cytotoxic agents.[8,9] Aβ oligomers have been shown to disrupt cellular membranes, pointing to a possible toxic pathway.[10,11]

While most studies have focused on extracellular Aβ, the peptide has been also identified inside cells, specifically in neuronal mitochondria of AD patients,[12] and in animal models.[13,14] Intracellular accumulation of Aβ occurs through two main pathways, specifically APP cleavage in the Golgi network, endoplasmic reticulum, and mitochondrial membranes[15,16] and insertion of Aβ through membrane pores and other molecular uptake processes.[17] Aβ has been shown to translocate through the outer mitochondrial membrane (OMM) and was consequently found within the mitochondrial cristae and in the inner mitochondrial membrane.[18] Indeed, mitochondrial dysfunction has been related to the pathological features of AD.[19]

The B-cell lymphoma 2 (Bcl-2) protein family plays a pivotal role in apoptosis regulation. These proteins, comprising the Bcl-2 homology (BH) domains, exhibit either proapoptotic or antiapoptotic functions and regulate apoptosis through intricate mechanisms.[20] The proapoptotic Bcl-2 proteins are further divided into two groups. The multiregion proteins Bax, Bak, and Bok share the BH 1−4 domains and generally disrupt mitochondrial membrane potential inducing leakage of cytochrome C (Cyt-C).[21] The second grouping, BH3-only proteins which include BIM, BID, PUMA, BAD, and NOXA are prominent initiators of apoptosis pathways originating in the mitochondria.[22,23] These proteins inhibit the activity of antiapoptotic counterparts,[24] induce mitochondrial outer membrane permeabilization, and promote release of Cyt-C,

Received: September 15, 2021
Accepted: November 11, 2021

overall contributing to activation of caspase cascades mediating cell death pathways.[25]

BID, PUMA, and NOXA particularly are prominent proapoptotic Bcl-2 proteins (Table 1). BID, a nonselective proapoptotic peptide, is localized in the cytoplasm close to the OMM, binds Bax/Bak, and subsequently activates caspase-8, which transforms BID into truncated BID leading to release of Cyt-C.[26] PUMA is also nonselective and mostly identified in the OMM, activating Bax and Bak by blocking antiapoptotic Bcl-2 proteins.[27] NOXA is an endogenous inhibitor of the antiapoptotic protein Mcl-1, thereby shifting cells toward apoptosis.[28]

Table 1. BH3 Peptides Motif Mapped on Key Proapoptotic Bcl-2 Proteins

		proapoptotic BH3-only motif
BID	82	I I R N I A R H L A Q V G D S M D R S I P P
PUMA	137	W A R E I G A Q L R R M A D D L N A Q Y E R
NOXA	21	L E V E C A T Q L R R F G D K L N F R Q K L

While the relationship between Aβ and mitochondrial dysfunction is not known, several reports have indicated elevated levels of Bcl-2 proteins in neuronal cells of AD patients.[29,30] A recent study provided intriguing evidence of structural and functional interplay between the proapoptotic BIM protein and Aβ42.[31] That report furnished the first evidence of a putative "crosstalk" between a proapoptotic peptide and Aβ42, pointing to possible physiological implications of such interactions. Here, we investigate the effects of the proapoptotic BID, PUMA, and NOXA on the structural and functional properties of Aβ42. Interestingly, we discovered significant, divergent effects of the three peptides upon the biological properties of Aβ42. While BID and PUMA are shown to accelerate Aβ42 fibrillation and reduce its cytotoxicity, NOXA reinforced formation of toxic oligomeric Aβ42 species. The presented results may reveal new mechanisms accounting for the toxic effects of the beta amyloid peptide and AD pathophysiology in general.

2. RESULTS AND DISCUSSION

2.1. BID, PUMA, and NOXA Affect Aβ42 Aggregation.

In this study, we investigate the impact of BID, PUMA, or NOXA upon the biological activities of Aβ42. We initially examined the effects of the proapoptotic peptides upon Aβ42 aggregation in buffer (Figure 1A) and in the presence of lipid vesicles mimicking the mitochondrial composition (Figure 1B). The thioflavin-T (ThT) fluorescence curves in Figure 1A,(i) attest to distinct, divergent impacts of the peptides upon the kinetics of Aβ42 fibrillation. ThT emission is widely employed for monitoring amyloid fibril formation.[32] The ThT fluorescence curve recorded in the presence of Aβ42 alone (Figure 1A,(i), gray curve) features a rapid emission increase and a plateau attained within ~4 h, reflecting the formation of mature fibrils.[33] Interestingly, both BID (Figure 1A,(i), green curve) and PUMA (Figure 1A,(i), black curve) enhanced the ThT signals compared to Aβ42 alone, likely pointing to more

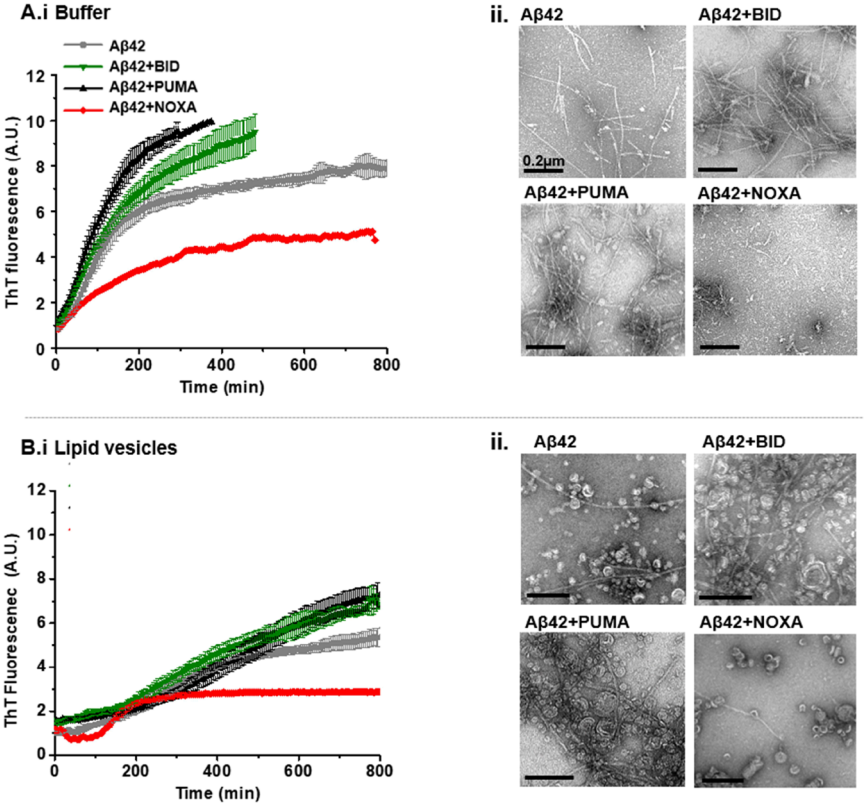

Figure 1. Modulation of Aβ42 fibrillation by BID, PUMA, and NOXA. (A) (i). Buffer measurements. (i) ThT fluorescence curves of Aβ42, recorded in buffer (gray curve) or in the presence of the peptides: BID (green), PUMA (black), and NOXA (red). Aβ42 concentration was 20 μM; BH3-only peptide concentrations were 40 μM. (ii). Transmission electron microscopy (TEM) images of the samples for which the ThT curves were recorded after 24 h incubation. (B) Vesicle solutions. (i) and (ii) depict ThT curves and TEM images recorded in the presence of lipid vesicles comprising DOPC/CL (90:10). The final vesicle concentration was 0.4 mM.

https://doi.org/10.1021/acschemneuro.1c00611
ACS Chem. Neurosci. XXXX, XXX, XXX−XXX

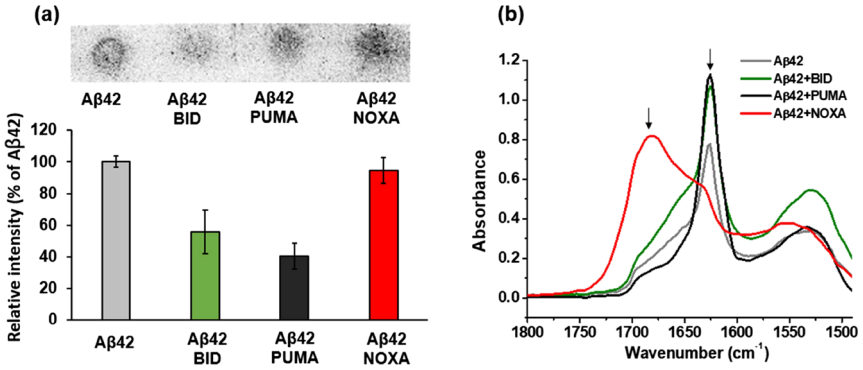

Figure 2. Modulation of Aβ42 oligomerization. (A) A11 dot blot assay for assessing the abundance of Aβ42 prefibril aggregates and oligomeric species. Top: Scanned image of the dot blots depicting Aβ42 alone or incubated with the BH3-only peptides for 4 h. Bottom: Dot intensities quantified by ImageJ software. (B) Fourier transform infrared (FTIR) spectra of Aβ42 alone (gray spectrum) or mixed with BID (green), PUMA (black), or NOXA (red). The arrows indicate the FTIR bands corresponding to β-sheets (1625 cm^{-1}) and Aβ42 oligomers (1695 cm^{-1}).

pronounced Aβ42 aggregation upon incubation with the two proapoptotic peptides (importantly, no ThT emission increase was recorded when the proapoptotic peptides were incubated alone in the buffer solutions, Figure 1,SI, indicating that neither peptide underwent aggregation).

In contrast to BID and PUMA, NOXA gave rise to significant reduction of the ThT fluorescence (Figure 1A, (i) red curve) likely indicating inhibition of Aβ42 fibril formation. The TEM images in Figure 1A, (ii) further attest to the divergent effects of BID, PUMA, and NOXA upon Aβ42 aggregation. Consistent with the ThT data in Figure 1A, (i), both BID and PUMA appeared to increase Aβ42 fibril abundance while NOXA inhibited fibril formation (Figure 1A, (ii) ThT fluorescence experiments (Figure 1B, (i) and TEM (Figure 1B, (ii) carried out in the presence of lipid vesicles comprising dioleyl-phosphatidylcholine (DOPC) and cardiolipin (CL) designed to mimic the mitochondrial membrane environment yielded qualitatively similar divergent effects of the proapoptotic peptides upon Aβ42 aggregation. The different ThT curve appearance and lower fluorescence emissions in the vesicle solutions (Figure 1B, (i) compared to buffer (e.g., Figure 1A, (i) are attributed to chaperoning of the Aβ42 peptides by free lipids in the aqueous phase,[34,35] thereby inhibiting protein−protein interactions and fibril formation.[36,37]

While Aβ42 fibrils are a major feature of AD, it has been hypothesized that Aβ42 oligomers and protofibrils constitute major toxic species.[38] Accordingly, we investigated the effects of the three proapoptotic peptides upon Aβ42 oligomer formation (Figure 2). Figure 2A depicts application of the A11 dot blot antibody assay[39] to assess the effects of BID, PUMA, and NOXA upon the relative abundance of Aβ42 oligomeric species. We particularly examined whether the effects of the peptides upon Aβ42 fibrillation (i.e., enhancement/inhibition, Figure 1A,B) were correlated with Aβ42 oligomer assembly. Indeed, the A11 results in Figure 2A attest to significantly lower concentrations of Aβ42 oligomers when Aβ42 was incubated with BID or PUMA, likely accounting for the accelerated formation of mature fibrils (observed in the ThT and TEM analyses, Figure 1A,B). Further echoing the aggregation data in Figure 1A,B, higher concentration of Aβ42 oligomers was recorded in the NOXA/Aβ42 mixture (Figure 2A), consistent with inhibition of the Aβ42 fibrillation process induced by NOXA.

We further analyzed the secondary structure of Aβ42 in the presence of the proapoptotic peptides by FTIR spectroscopy (Figure 2B). The FTIR spectrum of Aβ42 alone displays a prominent band at around 1625 cm^{-1} corresponding to β-sheets in mature fibrils (Figure 2B, gray).[40] Incubation of Aβ42 with BID or PUMA (for 24 h) gave rise to a similar spectral appearance, exhibiting a more intense peak at 1625 cm^{-1} (Figure 2B, green and black, respectively), likely reflecting the enhanced Aβ42 fibrillation induced by the two peptides (i.e., Figure 1A,B). Importantly, the FTIR spectrum of the Aβ42/NOXA mixture features a broad peak around 1695 cm^{-1} (Figure 2B, red) attributed to oligomeric species,[40,41] consistent with the abundance of NOXA-induced Aβ42 oligomers apparent in the A11 dot blot experiment (e.g., Figure 2A).

2.2. Effects of BID, PUMA, and NOXA on Membrane Interactions of Aβ42. Numerous studies have linked the toxic properties of Aβ42 to its membrane interactions, particularly of the oligomeric Aβ42 species.[42,43] Accordingly, we investigated the effects of BID, PUMA, and NOXA upon interactions of Aβ42 with biomimetic membrane bilayers (Figure 3). In particular, because the proapoptotic peptides are associated with the mitochondria we utilized vesicles comprising DOPC and CL—a negative lipid almost exclusively localized in mitochondrial membranes.[44] Figure 3A depicts the diffusion correlation time (τ_c) calculated from electron spin resonance (ESR) experiments carried out using CL/DOPC small unilamellar vesicles (SUVs) further comprising an *N*-tempoyl palmitamide (*N*-TEMPO) radical spin probe (the ESR spectra are presented in Figure 2,SI). Previous ESR studies employing *N*-TEMPO/lipid vesicles have provided useful information on the dynamic properties and fluidity within lipid bilayers' head-group environments.[45,46]

Figure 3A indicates that the τ_c / τ_0 ratio was significantly decreased upon incubation of the *N*-TEMPO/CL/DOPC vesicles with Aβ42, ascribed to the disruption of lipid bilayers by the peptide and concomitant increased fluidity of the *N*-TEMPO spin probe.[45,46] Notably, all three proapoptotic peptides modulated bilayer interactions when coincubated with Aβ42 (Figure 3A). In particular, when BID and PUMA were coadded to the lipid vesicles together with Aβ42, the diffusion correlation times significantly increased compared to Aβ42 alone, yielding τ_c / τ_0 values that were close to the control *N*-TEMPO/PC/CL vesicles (without addition of Aβ42). This result is consistent with the inhibition of Aβ42 oligomer

https://doi.org/10.1021/acschemneuro.1c00611
ACS Chem. Neurosci. XXXX, XXX, XXX−XXX

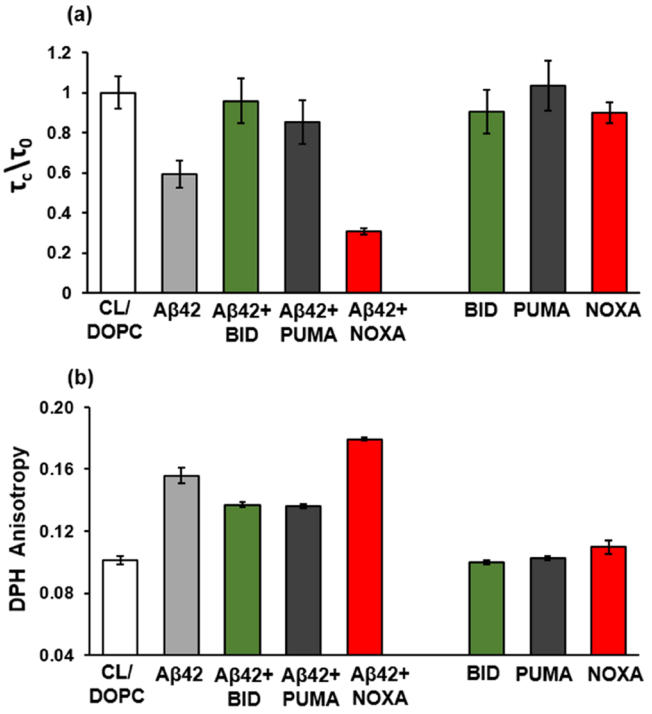

Figure 3. Modulation of Aβ42-membrane interactions by BIS, PUMA, or NOXA. (A) Changes in diffusion correlation time (τ_c) ratios calculated from the ESR spectra recorded for *N*-TEMPO in CL/DOPC (1:9) SUVs. All results are normalized according to the measurements of CL/DOPC vesicles alone indicated by τ_0. (B) Fluorescence anisotropy recorded in diphenylhexatriene (DPH)-doped CL/DOPC vesicles. Results are presented as means ± standard error of the mean (SEM) using nine replicates. In both ESR and anisotropy experiments, Aβ42 concentration was 20 μM and BH3-only peptide concentrations were 40 μM.

formation (Figure 2). In contrast to the "membrane shielding" effect of BID and PUMA, Figure 3A reveals that coaddition of NOXA and Aβ42 gave rise to short diffusion correlation time ($\tau_c/\tau_0 = 0.3$), a value that was even lower than the one induced by Aβ42 alone ($\tau_c/\tau_0 = 0.6$). The enhanced bilayer fluidity corroborates the recorded generation of higher abundance of membrane-active Aβ42 oligomers by NOXA (e.g., Figure 2). It should be noted that the proapoptotic peptides alone did not induce experimentally significant changes in bilayer fluidity (bars on the right in Figure 3A).

Fluorescence anisotropy experiments, presented in Figure 3B, further illuminate the effects of BID, PUMA, or NOXA upon membrane interactions of Aβ42. The bar diagram in Figure 3B shows the fluorescence anisotropy values of DPH embedded within CL/DOPC vesicles (1:500 ratio) following addition of Aβ42 or Aβ42/proapoptotic peptide mixtures. Fluorescence anisotropy analyses of bilayer-embedded DPH have been previously employed as a sensitive measure of lipid fluidity and the effect of membrane-active molecules upon bilayer dynamics.[47] Figure 3B indicates that Aβ42 induced higher fluorescence anisotropy in the DPH/CL/DOPC bilayers because of membrane interactions of the peptide oligomers.[31,48] In comparison, both the Aβ42/BID and Aβ42/PUMA mixtures gave rise to lesser anisotropy increase compared to Aβ42 alone, reflecting less pronounced membrane interactions apparent also in the ESR analysis (e.g., Figure 3A).

The Aβ42/NOXA mixture, on the other hand, yielded increased DPH anisotropy reflecting significant penetration of the abundant Aβ42 oligomers into the bilayer thereby restricting lipid motion. This result is consistent with the reduced mobility of the *N*-TEMPO spin probe displayed at the bilayer surface (e.g., Figure 3A) as both measurements account for the more pronounced bilayer interactions of the NOXA-induced Aβ42 oligomers. It should be noted that no significant changes in DPH fluorescence anisotropy were observed when BID, PUMA, or NOXA was added individually to the DPH/CL/DOPC vesicles (Figure 3B).

Significant membrane interactions and bilayer disruption are considered major determinants of Aβ42 prefibrillar assemblies,[49] and oligomer/lipid bilayer interactions have been implicated in the cytotoxic features of Aβ42.[50,51] Aβ has been shown to interact with lipid membranes either through insertion into the bilayer and formation of pore-like structures[52,53] or through binding and disruption of the bilayer surface.[54,55] The ESR and fluorescence anisotropy data in Figure 3, employing CL/phospholipid vesicles mimicking mitochondrial membranes, attest to more pronounced bilayer fluidity induced by coaddition of NOXA and Aβ42, while the opposite (bilayer rigidity) was observed when BID or PUMA was coincubated with Aβ42 prior to addition of the lipid vesicles. These results are consistent with the higher abundance of Aβ42 oligomeric and prefibrillar species when the peptide was incubated with NOXA, while the lower Aβ42 oligomer concentrations (going hand in hand with enhanced fibrillation) may account for the reduced membrane activity of Aβ42 upon addition of BID or PUMA.

The divergent effects of BID/PUMA versus NOXA on Aβ42 structural and functional properties are intriguing. These differences may be traced to the observation that NOXA exhibits selectivity toward its cellular protein targets, as compared to BID and PUMA which are believed to be nonselective in their interactions with their protein counterparts.[56] Indeed, several studies indicated that the BH3 domain in NOXA participates not only in binding and activation of proapoptotic proteins is pertinent cascades but is also involved in mitochondrial targeting and localization.[57,58] The amino acid sequence of NOXA may be further conducive to distinct interactions with Aβ42 as the presence of domains comprising alternating hydrophobic/hydrophilic residues within NOXA (i.e., LEVE...TQLR...LNFR...) could promote binding to beta-sheet regions within Aβ42.[59]

2.3. BID, PUMA, and NOXA Modulate Biological Activities of Aβ42. Beta amyloid aggregation, particularly the formation of Aβ42 oligomeric species, has been widely associated with neuronal toxicity and pathophysiological phenomena in AD.[60] Accordingly, we tested the effects of BID, PUMA, or NOXA upon Aβ42-induced cell death (Figure 4). Figure 4 depicts a SYTOX-annexin-V flow cytometry live/dead cell assay utilizing SH-SY5Y neuroblastoma cells. Aβ42 alone exhibited a significant toxic effect, giving rise to apoptosis (23.5% of cells underwent early and late apoptosis vs 8.7% in the case of control cells untreated with Aβ42; see the bar diagram in Figure 4B). Importantly, incubating the SH-SY5Y cells with Aβ42 and BID together or with the Aβ42/PUMA mixture significantly inhibited Aβ42-induced cell toxicity, significantly reducing the percentage of apoptotic cells (14.1 and 14.7% in the case of Aβ42/BID and Aβ42/PUMA, respectively, Figure 4B). The reduced apoptotic effects recorded for Aβ42/BID and Aβ42/PUMA are consistent

https://doi.org/10.1021/acschemneuro.1c00611
ACS Chem. Neurosci. XXXX, XXX, XXX−XXX

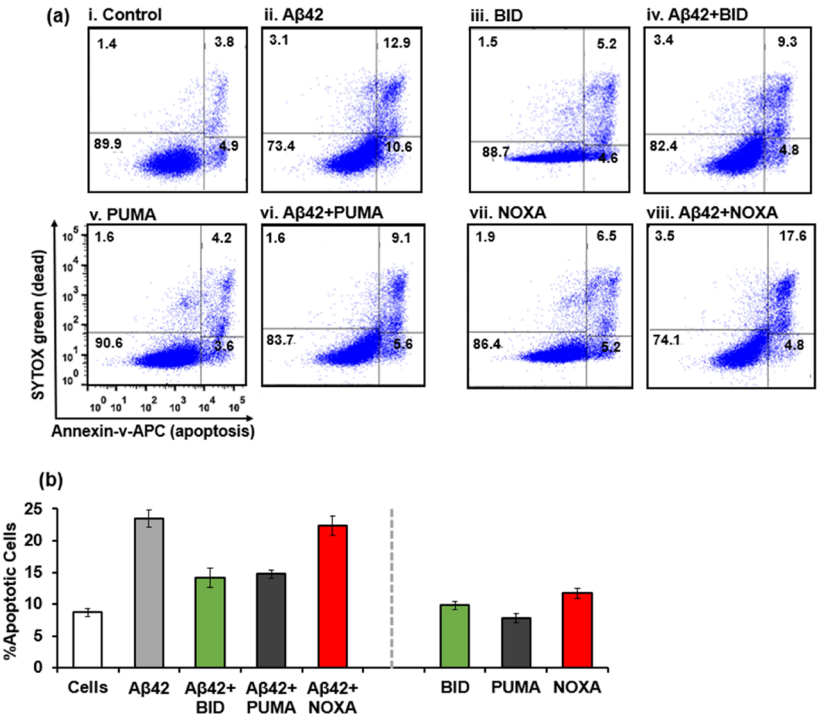

Figure 4. Effects of BID, PUMA, and NOXA upon Aβ42-induced cell apoptosis. SH-SY5Y cells were incubated with 15 μM Aβ42 in the presence or absence of the peptides (30 μM) for 24 h. (A) SYTOX-annexin V fluorescently activated cell sorting (FACS) data. The values in each quarter (gate) represent the percentage of cells in healthy state (bottom left) necrotic (top left), early apoptotic (bottom right), and late apoptosis (top right). (B) Percentage of early + late apoptotic cells determined in the FACS analysis. Data were collected in triplicate, depicting average ± SD.

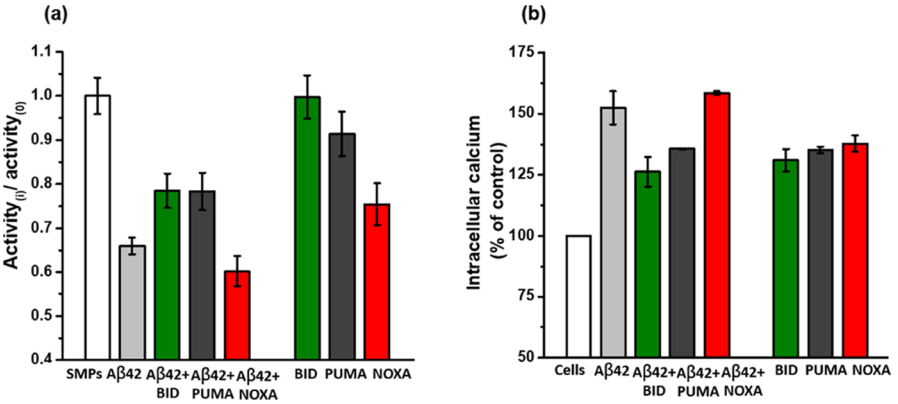

Figure 5. Aβ42 effects upon mitochondria functionalities with and without coaddition of BID, PUMA, or NOXA. (A) COX activity assay; SMPs were treated with Aβ42 alone (15 μM), or Aβ42 (15 μM) together with BID, PUMA, or NOXA (all peptides at 30 μM). COX absorbance was recorded at 550 nm in the presence of the ferrocytochrome c substrate (0.22 mM). Activity$_{(0)}$ corresponds to the enzyme activity in SMPs alone while activity$_{(i)}$ corresponds to enzyme activity in SMPs mixed with the peptides. All results were normalized according to the control measurement, that is, activity of COX in SMPs alone. (B) Intracellular calcium levels in SH-SY5Y cells. Cells were incubated with Aβ42 alone (15 μM) or Aβ42 together with BID, PUMA, or NOXA (all peptides at 30 μM) for 48 h. Calcium levels were determined using the Fluo-4 direct assay (see the Experimental section). Intracellular calcium in untreated cells was used as the control.

with the accelerated Aβ42 fibrillation and lower abundance of the cytotoxic Aβ42 oligomers induced by the proapoptotic peptides in the presence of lipid vesicles (Figure 1B).

Incubating the SH-SY5Y cells with a mixture of Aβ42 and NOXA had a significantly higher toxic effect compared to Aβ42/BID or Aβ42/PUMA, yielding apoptotic cell population at around 22%, similar to Aβ42 alone (Figure 4B). This result is consistent with the fibrillation analysis in Figure 1, which indicated that NOXA gave rise to lesser formation of mature Aβ42 fibrils and greater abundance of the putatively toxic Aβ42 oligomers. Additional cell viability experiments (using the XTT assay, Figure 3,SI) yielded toxicity profiles that were similar to the FACS analysis for the BID/Aβ42, PUMA/Aβ42, and NOXA/Aβ42 mixtures. Indeed, the experimental data in Figure 4 show a high cytotoxic effect induced upon incubating SH-SY5Y cells with NOXA/Aβ42, while the fibrillar mix of BID/Aβ42 or PUMA/Aβ42 featured significant less cytotoxicity. It is important to note that limitations of the in vitro study do exist, including molecular crowding within the cells and the presence of varied intracellular lipids or other proteins that may alter an effect of Aβ42 aggregation in the environment of the live cells.

While Figure 4 illustrates the effect of the BH3-only peptides upon cell viability, we further investigated whether the

https://doi.org/10.1021/acschemneuro.1c00611
ACS Chem. Neurosci. XXXX, XXX, XXX−XXX

proapoptotic peptides also modulated the effect of Aβ42 upon mitochondrial functionalities, because mitochondria constitute the primary cellular environments in which these proapoptotic peptides function[58] (Figure 5). Figure 5A depicts the effects of Aβ42 or Aβ42/BH3-only peptide mixtures upon the enzymatic action of cytochrome C oxidase (COX). COX plays an important role in mitochondrial respirometry functions.[61] In the experiments depicted in Figure 5A, we isolated mitochondria from SH-SY5Y cells and prepared inside-out oriented submitochondrial particles (SMPs).[62] The SMPs allow exposure of the inner mitochondrial membrane, thereby enabling to determine COX activity.

Figure 5A shows that Aβ42 dramatically attenuated COX activity compared to the control SMPs. Indeed, previous studies have shown reduced activity of the enzyme in AD patients.[63] Notably, both BID and PUMA gave rise to higher COX activity when mixed with Aβ42 compared to Aβ42 alone echoing the cytotoxicity analysis (e.g., Figure 4) which showed lower cytotoxicity upon addition of BID or PUMA to Aβ42. In contrast, Figure 5A demonstrates that the NOXA/Aβ42 mixture further reduced COX enzymatic activity. Indeed, the COX activity assay in Figure 5A attests to "protective" effects of BID and PUMA when coincubated with Aβ42, while NOXA appears to enhance the adverse effect of Aβ42 upon COX functionality. The bar diagram in Figure 5A also confirms that modulation of COX activity by the Aβ42/peptide mixtures is not traced to the effects of the BH3-only peptides alone.

Figure 5B presents assessment of intracellular calcium release, furnishing additional insight into the impacts of Aβ42 and its mixture with BID, PUMA, or NOXA, upon mitochondrial functionality. Elevated intracellular calcium levels in neuronal cells are associated with Aβ42-induced cell toxicity.[64] Figure 5B shows that Aβ42 alone induced a significant increase in intracellular calcium concentration in SH-SH5Y cells (~60% higher Ca^{2+} level than the untreated cells). This result has been previously linked to the apoptotic and toxic effects of Aβ42.[64] Experimentally significant lower intracellular calcium levels were recorded, however, when BID or PUMA was coincubated with Aβ42 and added to the cells (Figure 5B), echoing the COX experiments in Figure 5A and similarly demonstrating that BID and PUMA reduced the adverse impact of Aβ42 upon mitochondrial functionality. Importantly, addition of the Aβ42-NOXA mixture to the SH-SH5Y cells gave rise to calcium release that was on par as Aβ42 alone, reflecting the significant difference between the toxicity-promoting effect of NOXA on the one hand and "shielding" action of BID and PUMA, on the other hand. The increase in Ca^{2+} release induced by BID, PUMA, or NOXA alone, compared to the control cells (Figure 5B, right), corresponds to their intrinsic proapoptotic functionalities.[65]

Mitochondrial dysfunction and release of proapoptotic factors such as cytochrome c are key events associated with neuronal cell death.[66] Previous studies reported localization of Aβ within the mitochondria and Aβ42-induced impairment of cellular respiration through inhibition of COX activity.[67] Indeed, both the COX assay and intercellular calcium release measurements (Figure 5) underscore the "protective" effects of BID and PUMA on the one hand and enhanced toxicity of NOXA on the other hand. In particular, while coaddition of Aβ42 and BID or PUMA hardly affected the activity of COX, enzymatic activity was significantly reduced upon addition of the NOXA/Aβ42 mixture, even more than Aβ42 alone (Figure 5A). NOXA similarly enhanced intracellular calcium release when coadded to Aβ42 to a greater degree than Aβ42 added individually (Figure 5B).

3. CONCLUSIONS

This study reports on distinct effects of the proapoptotic peptides BID, PUMA, and NOXA on the structural and functional properties of Aβ42. We found that incubation of Aβ42 with each of the three proapoptotic peptides modified Aβ42 aggregation, cytotoxicity, effects on mitochondrial functionalities, and membrane interactions. Interestingly, the peptides had markedly divergent effects upon Aβ42. In particular, BID and PUMA enhanced fibrillation of Aβ42, inhibited its membrane interactions, and reduced the adverse effects of Aβ42 upon cell viability and mitochondrial functions. NOXA, on the other hand, inhibited Aβ42 fibril formation, gave rise to greater Aβ42-induced cytotoxicity and mitochondrial damage, and exhibited greater membrane interactions. Overall, this study may underscore links between Aβ42 functionalities and toxic profile and intracellular secretion of proapoptotic peptides. Our observations may point to intriguing mechanisms by which proapoptotic proteins affect structural pathways and pathophysiology of intracellular Aβ42.

4. MATERIALS AND METHODS

4.1. Materials. Cytochrome c (equine heart), cytochrome c oxidase (bovine heart), DL-Dithiothreitol (DTT), ThT, and 1,1,1,3,3,3-hexafluoro-2-propanol (HFIP) were purchased from Sigma-Aldrich (Rehovot, Israel). CL (Heart, Bovine) sodium salt (CL), DOPC, and *N*-TEMPO were purchased from Avanti Polar Lipids Inc. (AL, USA). A calcium fluorometric assay kit was obtained from Biovision (CA, U.S.A), a Cell Proliferation Kit (XTT based) was purchased from biological industries (Beit Haemek, Israel), and an AnnexinV-APC/dead cell apoptosis kit was obtained from Invitrogen (CA, USA). A11 antioligomer antibody was obtained from Rhenium (Modi'in, Israel). Horseradish peroxidase-conjugated antirabbit IgG (HRP) was purchased from ZOTAL (Tel-Aviv, Israel).

4.2. Peptides. Aβ 1−42 (Aβ42) was purchased from Anaspec (CA, USA) in a lyophilized form at >95% purity. BID (amino acid sequence, single letter code: IIRNIARHLAQVGDSMDRSIPP), PUMA (WAREIGAQLRRMADDLNAQYER), and NOXA (LEVECATQLRRFGDKLNFRQKL) were purchased from GenScript (Hong Kong) at ≥95% purity. All peptides were not modified neither on the C-terminus nor the N-terminus; the peptides were used as received. Stock solutions of variant of BID, PUMA, and NOXA peptides were prepared at 0.5 mM in sterilized deionized water after autoclave and diluted into the solutions at the required concentrations.

4.3. Cell Cultures. Neuroblastoma cell lines (SH-SY5Y) were grown at 37 °C and in a 5% CO_2 atmosphere in Dulbecco's modified Eagle medium supplemented with 10% tetracycline-free fetal bovine serum, L-glutamine (2 mM), and penicillin (100 units/mL)/streptomycin (0.1 mg/mL) (Gibco, Israel).

4.4. Mitochondria Isolation. SH-SY5Y cells were harvested at 75−80% confluence. A mass of 1 g of cells pellet was rinsed with 10 mL of hypotonic solution (100 mM sucrose, 10 mM MOPS, pH 7.2, and 1 mM EGTA) to enable cells swell followed by an incubation of cells for 10 min on ice according to the protocol published earlier.[68] Two mL portions from the suspension were homogenized with a Teflon glass homogenizer by gentle circular strokes. Cell suspension was diluted with hypertonic solution (1.25 M sucrose, 10 mM MOPS, pH 7.2) in a ratio of 1 mL hypertonic solution per 10 mL cell suspension, to restore solution isotonicity. The cell aliquot was then diluted with six volumes of isolation buffer (75 mM mannitol, 225 mM sucrose, 10 mM MOPS, pH 7.2, 1 mM EGTA, and 0.1% fatty acid free BSA). Cellular detritus was precipitated at 2000 RPM, 4 °C for 5 min. The supernatant containing mitochondria was further centrifuged at 14,000 RPM, 4 °C for 25 min. The result of the

https://doi.org/10.1021/acschemneuro.1c00611
ACS Chem. Neurosci. XXXX, XXX, XXX−XXX

separation was a crude mitochondria pellet that was rinsed by centrifugation using the same conditions (14,000 RPM, 4 °C for 25 min) in 15 mL of MiR06 buffer (110 mM sucrose, 60 mM K-lactobionate, 20 mM HEPES, pH 7.2, 1 mM KH_2PO_4, 3 mM $MgCl_2 \times 6H_2O$, 0.5 mM EGTA, 20 mM taurine, and 0.1% fatty acid free BSA). The final pellet was resuspended in 100 μL MiR06 by vortexing and stored at −80 °C until use. Mitochondrial protein concentration (mg/ml) was determined by Bradford assay.

4.5. Preparation of SMPs. The SMPs were prepared according to the known protocol published elsewhere.[62] Isolated mitochondria extracted from SH-SY5Y cells were diluted with sonication buffer (250 mM sucrose, 10 mM Tris HCl, 1 mM EDTA, and pH 7.2) in a final volume of 2 mL. The mitochondria suspension was probe-sonicated for 30 s in ice using 20% amplitude and six cycles of 5 s on/off sonication, to form inside-out oriented SMPs (in which the inner mitochondrial membrane is facing out to the medium solution). The SMP solution was then centrifuged at 8000 RPM to remove large membranes remaining. SMP concentration (μg protein/mL) was determined by Bradford test. The inversion of the inner mitochondrial membrane in SMPs was verified by COX assay.

4.6. Preparation of SUVs. Lipid components of DOPC/CL (90:10) were dissolved in a mixture of chloroform/ethanol (1:1) and dried together in vacuum up to a constant weight followed by addition of sodium phosphate buffer (pH 7.4). Vesicles were freshly prepared by probe-sonication of the dried phospholipids for a duration of 10 min at room temperature, with 20% amplitude and on/off 59-sec cycles. The final total concentration of lipids was 1 mM for all experiments, except from the ESR experiment in which the final lipid concentration was 10 mM.

4.7. ThT Fluorescence Assay. ThT fluorescence measurements were conducted at 37 °C using a 96-well plate on a BioTek Synergy 4 microplate reader (Winooski, VT, USA). Measurements were performed using samples containing 20 μM Aβ42 in the absence or presence of 40 μM BID, PUMA, or NOXA. Here, 120 μL aliquots of the aggregation reaction were mixed with 10 μL of ThT (120 μM) in sodium phosphate buffer, pH 7.4 or in the presence of 0.4 mM lipid vesicles prepared from DOPC/CL (90:10) composition. Fluorescence intensity reading was performed every 6 min for a duration of 24 h. The fluorescence intensity was measured at λex = 440 and λem = 485 nm.

4.8. Transmission Electron Microscopy. Peptide aliquots (5 μL) from samples used in the ThT experiments were placed on 400-mesh copper grids covered with a carbon-stabilized Formvar film. Excess solutions were removed following 2 min of incubation, and the grids were negatively stained for 30 s with a 1% uranyl acetate solution. Samples were viewed in an FEI Tecnai 12 TWIN TEM instrument operating at 120 kV.

4.9. FTIR Spectroscopy. Samples containing Aβ42 (20 μM), BID, PUMA, or NOXA (40 μM) and their mixtures (1:2 molar ratio) were prepared by dissolving the proteins in a phosphate buffer and mixing in the appropriate ratios. Five microliter aliquots of the mixtures were transferred to aluminum-coated plates immediately after dissolution and after 24 h of incubation at 37 °C and dried under vacuum. FTIR spectra were recorded using an iN10 FTIR microscope (Thermo Fisher Scientific, USA) fitted with a liquid N2-S4 cooled mercury cadmium telluride A detector. Spectra were recorded in the range of 4000−675 cm^{-1}, at 4 cm^{-1} resolution, with 64 scans averaging and minimal measuring area of 30 × 30 μm.

4.10. A11 Dot Blot Assay. Oligomers of Aβ42 were prepared in the absence or presence of BID, PUMA, and NOXA peptides (molar ratios of Aβ42:peptide were 1:2) and probed by the oligomer-specific polyclonal antibody (pAb) A11 using a modification of previously described methods.[69] Briefly, Aβ42 was dissolved in HFIP solvent (221 μM) and further sonicated for 1 min. An aliquot of Aβ42 solution was dried to remove the organic solvent followed by dilution with 10 mM sodium phosphate buffer to a final peptide concentration of 15 μM. The resulting solutions were incubated at 37 °C for 4 h. Two microliter aliquots were applied on nitrocellulose membranes blocked for 1 h with 5% of nonfat milk in 10 mM Tris-buffered saline (TBS) followed by incubation with A11 at 1:1000 dilution in TBS containing 5% nonfat milk. Subsequently, an appropriate secondary horseradish peroxidase conjugant antirabbit IgG antibody was developed using an enhanced chemiluminescence reagent kit (GE Healthcare).

4.11. Flow Cytometry. For measuring the amounts of apoptotic cells, 1×10^5 of SH-SY5Y cells per well were seeded in a 24-well plate and treated with Aβ42 (15 μM) or mixtures of Aβ42 with BID, PUMA, or NOXA (Aβ42/peptide molar ratios were 1:2) incubated for 24 h. Prior to treatment, the samples were filtered through a 0.22 μm filter. The cells were subsequently harvested, resuspended in phosphate-buffered saline, and analyzed by FACS on a Beckman Gallios (Indianapolis, US). For apoptosis, an Annexin V-Allophycocyanin (APC) probe was used and for dead cell detection, the SYTOX green. Measurements were performed using the AnnexinV-APC/dead cell apoptosis kit (Invitrogen, Carlsbad, CA) according to the manufacturer protocol. Untreated SH-SY5Y cells served as the negative control.

4.12. COX Activity. COX activity was determined by monitoring the decrease in absorbance at 550 (nm) of chemically reduced ferrocytochrome c solution in the presence of SMPs (preparation protocol of the SMPs was outlined above). Ferrocytochrome c substrate solution (0.22 mM) was prepared by addition of 5 μM DTT (0.1 M) to 2.7 mg/mL COX dissolved in purified water. Samples of SH-SY5Y SMPs (500 μg/mL final concentration) were mixed with 15 μM Aβ42 or 30 μM of BID/PUMA/NOXA peptides or their mixtures (molar ratio of 2:1) after preincubation of 4 h. Each sample was supplemented with 950 μL of buffer (10 mM Tris HCl, 120 mM KCl, pH 7.0). Enzyme buffer (10 mM Tris HCl, 250 mM sucrose pH 7.0) was then added to complete the total reaction volume to 1.1 mL. To initiate the oxidation reaction between ferricytochrome c and COX, 50 μL of ferrocytochrome c substrate was added to the enzyme. Two hundred microliter aliquots were measured in five repeats using a 96-well plate. The kinetic changes of absorbance were measured for 20 min, with 20 s intervals at 25 °C on a BioTek Synergy 4 microplate reader (Winooski, VT, USA). The activity of COX (units/ml) was calculated according to the equation:

$$\text{COX activity}\left(\frac{\text{units}}{\text{mL}}\right) = \frac{\Delta A/\text{s} \times \text{dil} \times V(t)}{V(\text{s}) \times 21.84}$$

in which ΔA/sec represents the reaction rate of a sample subtracted from blank; dil refers to the dilution factor of ferrocytochrome c solution; $V(t)$, total reaction volume; $V(\text{s})$ is the volume of the ferrocytochrome c substrate added to initiate oxidation, and 21.84 is the extinction coefficient between ferrocytochrome c and ferricytochrome c at 550 nm.[70] Unit definition: One unit oxidizes 1.0 μmole of ferrocytochrome c per sec at pH 7.0, 25 °C.

4.13. Intracellular Calcium Release. For measuring intracellular calcium levels, 1×10^4 SH-SY5Y cells were seeded in each well in a black-clear bottom 96-well plate. Cells were treated with 15 μM Aβ42 in the absence or presence of 30 μM BID/PUMA/NOXA peptides for 48 h. The cells were subjected to the intracellular calcium assay using the Flou-4- direct calcium assay kit (Biovision), according to the manufacture protocol, which measures the increase in fluorescence relative to the nontreated control. Changes of the fluorescence emission were measured using a BioTek Synergy 4 microplate reader (Winooski, VT, USA) with fluorescence excitation and emission wavelengths of 494 and 516 nm, respectively.

4.14. Electron Spin Resonance. Samples for ESR experiments were prepared using the *N*-TEMPO radical spin probe. *N*-TEMPO was supplemented with 10 mM CL/DOPC (10:90 molar ratio) vesicles (10 mM) in a molar ratio of 500:1 (phospholipid/spin probe) followed by incubation of 20 min at 25 °C. Samples of Aβ42 (20 μM), BID/PUMA/NOXA peptides (40 μM), or mix of Aβ42 and peptides were incubated for 4 h and placed in a 20 mm length and 1 mm ID glass capillary. ESR spectra were recorded in triplicate using an EPR mini-X-band spectrometer (Spin Ltd., Russia) at room temperature. The modulation was 20G, and time constant 0.01 and the microwave power level were chosen at subcritical values of 20 mW

https://doi.org/10.1021/acschemneuro.1c00611
ACS Chem. Neurosci. XXXX, XXX, XXX−XXX

to obtain an optimal signal-to-noise ratio. Diffusion correlation time (τ_c) values were calculated from the ESR spectra using the equation:

$$\tau_c = 6.6 \times 10^{-10} \times \Delta H_{(+1)} \left(\sqrt{\frac{I_{(+1)}}{I_{(-1)}}} - 1 \right) (\text{sec})$$

in which τ_c is the diffusion correlation time (sec); 6.6×10^{-10} is the constant pertinent to the spin label; $\Delta H_{(+1)}$, is the low field line width; $I_{(+1)}$, is the low field line height and $I_{(-1)}$ is the highest field line height.

4.15. Fluorescence Anisotropy. The fluorescent probe DPH was incorporated into the SUVs (DOPC/CL 90:10 molar ratio) by adding the dye dissolved in THF (1 mg/mL) to vesicles in a molar ratio of 500:1 (lipid/probe). After 30 min of incubation at 30 °C, fluorescence anisotropy was measured at λex = 360 nm and λem = 430 nm on a Fluorolog spectrofluorometer (HORIBA, Japan). Data were collected before and after addition of freshly dissolved Aβ42, the proapoptotic peptides: BID, PUMA, NOXA, or their mixtures (molar ratio of 1:2). Anisotropy values were automatically calculated with the spectrofluorometer software using the equation:

$$r = \frac{(I_{VV} - GI_{VV})}{(I_{VV} - 2GI_{VH})}, \quad G = \frac{I_{VH}}{I_{HH}}$$

in which I_{VV} is the intensity with excitation and emission polarizers mounted vertically; I_{HH} corresponds to the excitation and emission polarizers mounted horizontally; I_{HV} is the excitation polarizer horizontal and the emission polarizer vertical; I_{VH} pertains to the excitation polarizer vertical and emission polarizer horizontal. Results are presented as means ± SEM of seven replicates.

■ ASSOCIATED CONTENT

Supporting Information

The Supporting Information is available free of charge at https://pubs.acs.org/doi/10.1021/acschemneuro.1c00611.

ThT control measurements for BH3-only peptides incubated in buffer; The original ESR spectra in which the $\tau\tau$c values calculated from and presented at figure 3A in main next; Cell toxicity of Aβ42 and BH3 peptides; HPLC and MS traces of the BID peptide; HPLC and MS traces of the PUMA peptide; HPLC and MS traces of the NOXA peptide (PDF)

■ AUTHOR INFORMATION

Corresponding Author

Raz Jelinek − *Department of Chemistry and Ilse Katz Institute for Nanotechnology, Ben Gurion University of the Negev, Beer Sheva 84105, Israel;* orcid.org/0000-0002-0336-1384; Email: razj@bgu.ac.il

Authors

Shani Ben-Zichri − *Department of Chemistry and Ilse Katz Institute for Nanotechnology, Ben Gurion University of the Negev, Beer Sheva 84105, Israel*

Ravit Malishev − *Department of Chemistry and Ilse Katz Institute for Nanotechnology, Ben Gurion University of the Negev, Beer Sheva 84105, Israel*

Ofek Oren − *The Shraga Segal Department of Microbiology, Immunology and Genetics, Faculty of Health Sciences, Ben-Gurion University of the Negev, Beer Sheva 84105, Israel*

Daniel N. Bloch − *Department of Chemistry and Ilse Katz Institute for Nanotechnology, Ben Gurion University of the Negev, Beer Sheva 84105, Israel*

Ran Taube − *The Shraga Segal Department of Microbiology, Immunology and Genetics, Faculty of Health Sciences, Ben-Gurion University of the Negev, Beer Sheva 84105, Israel*

Niv Papo − *Avram and Stella Goldstein-Goren Department of Biotechnology Engineering and the National Institute of Biotechnology, Ben-Gurion University of the Negev, Beer Sheva 84105, Israel;* orcid.org/0000-0002-7056-2418

Complete contact information is available at: https://pubs.acs.org/10.1021/acschemneuro.1c00611

Author Contributions

S.B.Z., R.M., and R.J. conceived the idea and designed the experiments; S.B.Z, R.M, O.O., and D.N.B. performed the research; S.B.Z., R.M., and R.J analyzed the data and wrote the manuscript. All authors edited the manuscript and approved the final version. S.B.Z. and R.M. contributed equally.

Notes

The authors declare no competing financial interest.

■ ACKNOWLEDGMENTS

We are grateful to Dr. Sofiya Kolusheva for helping with the fluorescence experiments.

■ ABBREVIATIONS

Aβ, amyloid beta; Bcl-2, B-cell lymphoma 2; BH3, Bcl-2 homology 3; BID, BH3 interacting-domain death agonist; CL, cardiolipin; COX, cytochrome c oxidase; Cyt-C, cytochrome C; DOPC, 1,2-dioleoyl-sn-glycero-3-phosphocholine; ESR, electron spin resonance; FTIR, Fourier transform infrared spectroscopy; *N*-TEMPO, *N*-tempoyl palmitamide; OMM, outer mitochondrial membrane; PUMA, p53 upregulated modulator of apoptosis; SMPs, submitochondrial particles; SUVs, small unilamellar vesicles; TEM, transmission electron microscopy; ThT, thioflavin T

■ REFERENCES

(1) Funamoto, S.; Tagami, S.; Okochi, M.; Morishima-Kawashima, M. Successive cleavage of beta-amyloid precursor protein by gamma-secretase. *Semin. Cell Dev. Biol.* **2020**, *105*, 64−74.

(2) Pantelopulos, G. A.; Straub, J. E.; Thirumalai, D.; Sugita, Y. Structure of APP-C991-99 and implications for role of extra-membrane domains in function and oligomerization. *Biochim. Biophys. Acta, Biomembr.* **2018**, *1860*, 1698−1708.

(3) Crews, L.; Masliah, E. Molecular mechanisms of neuro-degeneration in Alzheimer's disease. *Hum. Mol. Genet.* **2010**, *19*, R12−R20.

(4) Ivanova, M. I.; Lin, Y.; Lee, Y. H.; Zheng, J.; Ramamoorthy, A. Biophysical processes underlying cross-seeding in amyloid aggregation and implications in amyloid pathology. *Biophys. Chem.* **2021**, *269*, No. 106507.

(5) Sharma, S.; Modi, P.; Sharma, G.; Deep, S. Kinetics theories to understand the mechanism of aggregation of a protein and to design strategies for its inhibition. *Biophys. Chem.* **2021**, *278*, No. 106665.

(6) Romanucci, V.; Garcia-Vinuales, S.; Tempra, C.; Bernini, R.; Zarrelli, A.; Lolicato, F.; Milardi, D.; Di Fabio, G. Modulating Abeta aggregation by tyrosol-based ligands: The crucial role of the catechol moiety. *Biophys. Chem.* **2020**, *265*, No. 106434.

(7) Said, M. S.; Navale, G. R.; Yadav, A.; Khonde, N.; Shinde, S. S.; Jha, A. Effect of tert-alcohol functional imidazolium salts on oligomerization and fibrillization of amyloid beta (1-42) peptide. *Biophys. Chem.* **2020**, *267*, No. 106480.

(8) Sengupta, U.; Nilson, A. N.; Kayed, R. The Role of Amyloid-beta Oligomers in Toxicity, Propagation, and Immunotherapy. *EBioMedicine* **2016**, *6*, 42−49.

(9) Nguyen, P. H.; Ramamoorthy, A.; Sahoo, B. R.; Zheng, J.; Faller, P.; Straub, J. E.; Dominguez, L.; Shea, J. E.; Dokholyan, N. V.; De Simone, A.; Ma, B.; Nussinov, R.; Najafi, S.; Ngo, S. T.; Loquet, A.; Chiricotto, M.; Ganguly, P.; McCarty, J.; Li, M. S.; Hall, C.; Wang, Y.;

Miller, Y.; Melchionna, S.; Habenstein, B.; Timr, S.; Chen, J.; Hnath, B.; Strodel, B.; Kayed, R.; Lesne, S.; Wei, G.; Sterpone, F.; Doig, A. J.; Derreumaux, P. Amyloid Oligomers: A Joint Experimental/Computational Perspective on Alzheimer's Disease, Parkinson's Disease, Type II Diabetes, and Amyotrophic Lateral Sclerosis. *Chem. Rev.* **2021**, *121*, 2545−2647.

(10) Flagmeier, P.; De, S.; Michaels, T. C. T.; Yang, X.; Dear, A. J.; Emanuelsson, C.; Vendruscolo, M.; Linse, S.; Klenerman, D.; Knowles, T. P. J.; Dobson, C. M. Direct measurement of lipid membrane disruption connects kinetics and toxicity of Abeta42 aggregation. *Nat. Struct. Mol. Biol.* **2020**, *27*, 886−891.

(11) Grasso, G.; Lionello, C.; Stojceski, F. Highlighting the effect of amyloid beta assemblies on the mechanical properties and conformational stability of cell membrane. *J. Mol. Graph. Model.* **2020**, *100*, No. 107670.

(12) Hu, W.; Wang, Z.; Zheng, H. Mitochondrial accumulation of amyloid beta (Abeta) peptides requires TOMM22 as a main Abeta receptor in yeast. *J. Biol. Chem.* **2018**, *293*, 12681−12689.

(13) Caspersen, C.; Wang, N.; Yao, J.; Sosunov, A.; Chen, X.; Lustbader, J. W.; Xu, H. W.; Stern, D.; McKhann, G.; Yan, S. D. Mitochondrial Abeta: a potential focal point for neuronal metabolic dysfunction in Alzheimer's disease. *FASEB J.* **2005**, *19*, 2040−2041.

(14) Manczak, M.; Anekonda, T. S.; Henson, E.; Park, B. S.; Quinn, J.; Reddy, P. H. Mitochondria are a direct site of A beta accumulation in Alzheimer's disease neurons: implications for free radical generation and oxidative damage in disease progression. *Hum. Mol. Genet.* **2006**, *15*, 1437−1449.

(15) Umeda, T.; Tomiyama, T.; Sakama, N.; Tanaka, S.; Lambert, M. P.; Klein, W. L.; Mori, H. Intraneuronal amyloid beta oligomers cause cell death via endoplasmic reticulum stress, endosomal/lysosomal leakage, and mitochondrial dysfunction in vivo. *J. Neurosci. Res.* **2011**, *89*, 1031−1042.

(16) Cho, D. H.; Nakamura, T.; Fang, J.; Cieplak, P.; Godzik, A.; Gu, Z.; Lipton, S. A. S-nitrosylation of Drp1 mediates beta-amyloid-related mitochondrial fission and neuronal injury. *Science* **2009**, *324*, 102−105.

(17) Bharadwaj, P.; Solomon, T.; Malajczuk, C. J.; Mancera, R. L.; Howard, M.; Arrigan, D. W. M.; Newsholme, P.; Martins, R. N. Role of the cell membrane interface in modulating production and uptake of Alzheimer's beta amyloid protein. *Biochim. Biophys. Acta, Biomembr.* **2018**, *1860*, 1639−1651.

(18) Hansson Petersen, C. A.; Alikhani, N.; Behbahani, H.; Wiehager, B.; Pavlov, P. F.; Alafuzoff, I.; Leinonen, V.; Ito, A.; Winblad, B.; Glaser, E.; Ankarcrona, M. The amyloid beta-peptide is imported into mitochondria via the TOM import machinery and localized to mitochondrial cristae. *Proc. Natl. Acad. Sci. U. S. A.* **2008**, *105*, 13145−13150.

(19) Castellani, R.; Hirai, K.; Aliev, G.; Drew, K. L.; Nunomura, A.; Takeda, A.; Cash, A. D.; Obrenovich, M. E.; Perry, G.; Smith, M. A. Role of mitochondrial dysfunction in Alzheimer's disease. *J. Neurosci. Res.* **2002**, *70*, 357−360.

(20) Kelekar, A.; Thompson, C. B. Bcl-2-family proteins: the role of the BH3 domain in apoptosis. *Trends Cell Biol.* **1998**, *8*, 324−330.

(21) Lindsten, T.; Ross, A. J.; King, A.; Zong, W. X.; Rathmell, J. C.; Shiels, H. A.; Ulrich, E.; Waymire, K. G.; Mahar, P.; Frauwirth, K.; Chen, Y.; Wei, M.; Eng, V. M.; Adelman, D. M.; Simon, M. C.; Ma, A.; Golden, J. A.; Evan, G.; Korsmeyer, S. J.; MacGregor, G. R.; Thompson, C. B. The combined functions of proapoptotic Bcl-2 family members bak and bax are essential for normal development of multiple tissues. *Mol. Cell* **2000**, *6*, 1389−1399.

(22) Cheng, E. H.; Wei, M. C.; Weiler, S.; Flavell, R. A.; Mak, T. W.; Lindsten, T.; Korsmeyer, S. J. BCL-2, BCL-X(L) sequester BH3 domain-only molecules preventing BAX- and BAK-mediated mitochondrial apoptosis. *Mol. Cell* **2001**, *8*, 705−711.

(23) Happo, L.; Strasser, A.; Cory, S. BH3-only proteins in apoptosis at a glance. *J. Cell Sci.* **2012**, *125*, 1081−1087.

(24) Chipuk, J. E.; Fisher, J. C.; Dillon, C. P.; Kriwacki, R. W.; Kuwana, T.; Green, D. R. Mechanism of apoptosis induction by inhibition of the anti-apoptotic BCL-2 proteins. *Proc. Natl. Acad. Sci. U. S. A.* **2008**, *105*, 20327−20332.

(25) Green, D. R.; Kroemer, G. The pathophysiology of mitochondrial cell death. *Science* **2004**, *305*, 626−629.

(26) Brustovetsky, N.; Dubinsky, J. M.; Antonsson, B.; Jemmerson, R. Two pathways for tBID-induced cytochrome c release from rat brain mitochondria: BAK- versus BAX-dependence. *J. Neurochem.* **2003**, *84*, 196−207.

(27) Yee, K. S.; Wilkinson, S.; James, J.; Ryan, K. M.; Vousden, K. H. PUMA- and Bax-induced autophagy contributes to apoptosis. *Cell Death Differ.* **2009**, *16*, 1135−1145.

(28) Oda, E.; Ohki, R.; Murasawa, H.; Nemoto, J.; Shibue, T.; Yamashita, T.; Tokino, T.; Taniguchi, T.; Tanaka, N. Noxa, a BH3-only member of the Bcl-2 family and candidate mediator of p53-induced apoptosis. *Science* **2000**, *288*, 1053−1058.

(29) Engidawork, E.; Gulesserian, T.; Seidl, R.; Cairns, N.; Lubec, G. Expression of apoptosis related proteins in brains of patients with Alzheimer's disease. *Neurosci. Lett.* **2001**, *303*, 79−82.

(30) Yao, M.; Nguyen, T. V.; Pike, C. J. Estrogen regulates Bcl-w and Bim expression: role in protection against beta-amyloid peptide-induced neuronal death. *J. Neurosci.* **2007**, *27*, 1422−1433.

(31) Malishev, R.; Nandi, S.; Smilowicz, D.; Bakavayev, S.; Engel, S.; Bujanover, N.; Gazit, R.; Metzler-Nolte, N.; Jelinek, R. Interactions between BIM Protein and Beta-Amyloid May Reveal a Crucial Missing Link between Alzheimer's Disease and Neuronal Cell Death. *ACS Chem. Nerosci.* **2019**, *10*, 3555−3564.

(32) Hudson, S. A.; Ecroyd, H.; Kee, T. W.; Carver, J. A. The thioflavin T fluorescence assay for amyloid fibril detection can be biased by the presence of exogenous compounds. *FEBS J.* **2009**, *276*, 5960−5972.

(33) Tran, J.; Chang, D.; Hsu, F.; Wang, H.; Guo, Z. Cross-seeding between Abeta40 and Abeta42 in Alzheimer's disease. *FEBS Lett.* **2017**, *591*, 177−185.

(34) Scollo, F.; Tempra, C.; Lolicato, F.; Sciacca, M. F. M.; Raudino, A.; Milardi, D.; La Rosa, C. Phospholipids Critical Micellar Concentrations Trigger Different Mechanisms of Intrinsically Disordered Proteins Interaction with Model Membranes. *J. Phys. Chem. Lett.* **2018**, *9*, 5125−5129.

(35) Sciacca, M. F.; Lolicato, F.; Tempra, C.; Scollo, F.; Sahoo, B. R.; Watson, M. D.; Garcia-Vinuales, S.; Milardi, D.; Raudino, A.; Lee, J. C.; Ramamoorthy, A.; La Rosa, C. Lipid-Chaperone Hypothesis: A Common Molecular Mechanism of Membrane Disruption by Intrinsically Disordered Proteins. *ACS Chem. Nerosci.* **2020**, *11*, 4336−4350.

(36) Korshavn, K. J.; Satriano, C.; Lin, Y.; Zhang, R.; Dulchavsky, M.; Bhunia, A.; Ivanova, M. I.; Lee, Y. H.; La Rosa, C.; Lim, M. H.; Ramamoorthy, A. Reduced Lipid Bilayer Thickness Regulates the Aggregation and Cytotoxicity of Amyloid-beta. *J. Biol. Chem.* **2017**, *292*, 4638−4650.

(37) Milardi, D.; Gazit, E.; Radford, S. E.; Xu, Y.; Gallardo, R. U.; Caflisch, A.; Westermark, G. T.; Westermark, P.; Rosa, C.; Ramamoorthy, A. Proteostasis of Islet Amyloid Polypeptide: A Molecular Perspective of Risk Factors and Protective Strategies for Type II Diabetes. *Chem. Rev.* **2021**, *121*, 1845−1893.

(38) Haass, C.; Selkoe, D. J. Soluble protein oligomers in neurodegeneration: lessons from the Alzheimer's amyloid beta-peptide. *Nat. Rev. Mol. Cell Biol.* **2007**, *8*, 101−112.

(39) Kayed, R.; Head, E.; Thompson, J. L.; McIntire, T. M.; Milton, S. C.; Cotman, C. W.; Glabe, C. G. Common structure of soluble amyloid oligomers implies common mechanism of pathogenesis. *Science* **2003**, *300*, 486−489.

(40) Cerf, E.; Sarroukh, R.; Tamamizu-Kato, S.; Breydo, L.; Derclaye, S.; Dufrene, Y. F.; Narayanaswami, V.; Goormaghtigh, E.; Ruysschaert, J. M.; Raussens, V. Antiparallel beta-sheet: a signature structure of the oligomeric amyloid beta-peptide. *Biochem. J.* **2009**, *421*, 415−423.

(41) Zou, Y.; Li, Y.; Hao, W.; Hu, X.; Ma, G. Parallel beta-sheet fibril and antiparallel beta-sheet oligomer: new insights into amyloid

https://doi.org/10.1021/acschemneuro.1c00611
ACS Chem. Neurosci. XXXX, XXX, XXX−XXX

formation of hen egg white lysozyme under heat and acidic condition from FTIR spectroscopy. *J. Phys. Chem. B* **2013**, *117*, 4003−4013.
(42) Malishev, R.; Nandi, S.; Kolusheva, S.; Levi-Kalisman, Y.; Klarner, F. G.; Schrader, T.; Bitan, G.; Jelinek, R. Toxicity inhibitors protect lipid membranes from disruption by Abeta42. *ACS Chem. Nerosci.* **2015**, *6*, 1860−1869.
(43) Valincius, G.; Heinrich, F.; Budvytyte, R.; Vanderah, D. J.; McGillivray, D. J.; Sokolov, Y.; Hall, J. E.; Losche, M. Soluble amyloid beta-oligomers affect dielectric membrane properties by bilayer insertion and domain formation: implications for cell toxicity. *Biophys. J.* **2008**, *95*, 4845−4861.
(44) Houtkooper, R. H.; Vaz, F. M. Cardiolipin, the heart of mitochondrial metabolism. *Cell. Mol. Life Sci.* **2008**, *65*, 2493−2506.
(45) Oren, O.; Ben Zichri, S.; Taube, R.; Jelinek, R.; Papo, N. Abeta42 Double Mutant Inhibits Abeta42-Induced Plasma and Mitochondrial Membrane Disruption in Artificial Membranes, Isolated Organs, and Intact Cells. *ACS Chem. Nerosci.* **2020**, *11*, 1027−1037.
(46) Sunamoto, J.; Akiyoshi, K.; Kihara, T.; Endo, M. A Water-Soluble Spin Probe Newly Developed for Liposomal Studies. *B Chem. Soc. Jpn* **1992**, *65*, 1041−1046.
(47) Suzuki, M.; Miura, T. Effect of amyloid beta-peptide on the fluidity of phosphatidylcholine membranes: Uses and limitations of diphenylhexatriene fluorescence anisotropy. *Biochim. Biophys. Acta* **2015**, *1848*, 753−759.
(48) Matveeva, E. G.; Rudolph, A.; Moll, J. R.; Thompson, R. B. Structure-selective anisotropy assay for amyloid Beta oligomers. *ACS Chem. Nerosci.* **2012**, *3*, 982−987.
(49) Cecchi, C.; Stefani, M. The amyloid-cell membrane system. The interplay between the biophysical features of oligomers/fibrils and cell membrane defines amyloid toxicity. *Biophys. Chem.* **2013**, *182*, 30−43.
(50) Chang, C. C.; Edwald, E.; Veatch, S.; Steel, D. G.; Gafni, A. Interactions of amyloid-beta peptides on lipid bilayer studied by single molecule imaging and tracking. *Biochim. Biophys. Acta, Biomembr.* **2018**, *1860*, 1616−1624.
(51) Kayed, R.; Lasagna-Reeves, C. A. Molecular mechanisms of amyloid oligomers toxicity. *J. Alzheimers Dis.* **2013**, *33*, S67−S78.
(52) Prangkio, P.; Yusko, E. C.; Sept, D.; Yang, J.; Mayer, M. Multivariate analyses of amyloid-beta oligomer populations indicate a connection between pore formation and cytotoxicity. *PLoS One* **2012**, *7*, No. e47261.
(53) Cox, S. J.; Lam, B.; Prasad, A.; Marietta, H. A.; Stander, N. V.; Joel, J. G.; Sahoo, B. R.; Guo, F.; Stoddard, A. K.; Ivanova, M. I.; Ramamoorthy, A. High-Throughput Screening at the Membrane Interface Reveals Inhibitors of Amyloid-beta. *Biochemistry* **2020**, *59*, 2249−2258.
(54) Connelly, L.; Jang, H.; Arce, F. T.; Capone, R.; Kotler, S. A.; Ramachandran, S.; Kagan, B. L.; Nussinov, R.; Lal, R. Atomic force microscopy and MD simulations reveal pore-like structures of all-D-enantiomer of Alzheimer's beta-amyloid peptide: relevance to the ion channel mechanism of AD pathology. *J. Phys. Chem. B* **2012**, *116*, 1728−1735.
(55) Wong, P. T.; Schauerte, J. A.; Wisser, K. C.; Ding, H.; Lee, E. L.; Steel, D. G.; Gafni, A. Amyloid-beta membrane binding and permeabilization are distinct processes influenced separately by membrane charge and fluidity. *J. Mol. Biol.* **2009**, *386*, 81−96.
(56) Ren, D.; Tu, H. C.; Kim, H.; Wang, G. X.; Bean, G. R.; Takeuchi, O.; Jeffers, J. R.; Zambetti, G. P.; Hsieh, J. J.; Cheng, E. H. BID, BIM, and PUMA are essential for activation of the BAX- and BAK-dependent cell death program. *Science* **2010**, *330*, 1390−1393.
(57) Ploner, C.; Kofler, R.; Villunger, A. Noxa: at the tip of the balance between life and death. *Oncogene* **2008**, *27*, S84−S92.
(58) Seo, Y. W.; Shin, J. N.; Ko, K. H.; Cha, J. H.; Park, J. Y.; Lee, B. R.; Yun, C. W.; Kim, Y. M.; Seol, D. W.; Kim, D. W.; Yin, X. M.; Kim, T. H. The molecular mechanism of Noxa-induced mitochondrial dysfunction in p53-mediated cell death. *J. Biol. Chem.* **2003**, *278*, 48292−48299.
(59) Cheng, R. P.; Gellman, S. H.; DeGrado, W. F. beta-Peptides: from structure to function. *Chem. Rev.* **2001**, *101*, 3219−3232.
(60) Wirths, O.; Multhaup, G.; Bayer, T. A. A modified beta-amyloid hypothesis: intraneuronal accumulation of the beta-amyloid peptide–the first step of a fatal cascade. *J. Neurochem.* **2004**, *91*, 513−520.
(61) Fontanesi, F.; Soto, I. C.; Horn, D.; Barrientos, A. Assembly of mitochondrial cytochrome c-oxidase, a complicated and highly regulated cellular process. *Am. J. Physiol. Cell Physiol.* **2006**, *291*, C1129−C1147.
(62) Lee, C. Tightly coupled beef heart submitochondrial particles. *Methods Enzymol.* **1979**, *55*, 105−112.
(63) Cardoso, S. M.; Proenca, M. T.; Santos, S.; Santana, I.; Oliveira, C. R. Cytochrome c oxidase is decreased in Alzheimer's disease platelets. *Neurobiol. Aging* **2004**, *25*, 105−110.
(64) Kawahara, M.; Kuroda, Y. Molecular mechanism of neurodegeneration induced by Alzheimer's beta-amyloid protein: channel formation and disruption of calcium homeostasis. *Brain Res. Bull.* **2000**, *53*, 389−397.
(65) Lomonosova, E.; Chinnadurai, G. BH3-only proteins in apoptosis and beyond: an overview. *Oncogene* **2008**, *27*, S2−S19.
(66) Landshamer, S.; Hoehn, M.; Barth, N.; Duvezin-Caubet, S.; Schwake, G.; Tobaben, S.; Kazhdan, I.; Becattini, B.; Zahler, S.; Vollmar, A.; Pellecchia, M.; Reichert, A.; Plesnila, N.; Wagner, E.; Culmsee, C. Bid-induced release of AIF from mitochondria causes immediate neuronal cell death. *Cell Death Differ.* **2008**, *15*, 1553−1563.
(67) Rhein, V.; Baysang, G.; Rao, S.; Meier, F.; Bonert, A.; Muller-Spahn, F.; Eckert, A. Amyloid-beta leads to impaired cellular respiration, energy production and mitochondrial electron chain complex activities in human neuroblastoma cells. *Cell. Mol. Neurobiol.* **2009**, *29*, 1063−1071.
(68) Panov, A. V.; Lund, S.; Greenamyre, J. T. Ca2+−induced permeability transition in human lymphoblastoid cell mitochondria from normal and Huntington's disease individuals. *Mol. Cell. Biochem.* **2005**, *269*, 143−152.
(69) Necula, M.; Kayed, R.; Milton, S.; Glabe, C. G. Small molecule inhibitors of aggregation indicate that amyloid beta oligomerization and fibrillization pathways are independent and distinct. *J. Biol. Chem.* **2007**, *282*, 10311−10324.
(70) Berry, E. A.; Trumpower, B. L. Simultaneous determination of hemes a, b, and c from pyridine hemochrome spectra. *Anal. Biochem.* **1987**, *161*, 1−15.

https://doi.org/10.1021/acschemneuro.1c00611
ACS Chem. Neurosci. XXXX, XXX, XXX−XXX